Jour. of the KGS, Vol. 18, No. 3. June 2002, pp. 87~94

An Experimental Study of the Soil Nailed Wall Behavior with Front Plate Rigidity

전면벽체 강성에 따른 쏘일네일링 벽체의 거동특성에 관한 실험적 고찰

Kim, Hong-Taek[*1] 김 홍 택 Kang, In-Kyu[*2] 강 인 규
Kwon, Young-Ho[*3] 권 영 호 Park, Si-Sam[*4] 박 시 삼
Cho, Yong-Hoon[*5] 조 용 훈

요 지

최근 들어 국내에서는 경제적이고 효율적인 지하굴착공법으로 쏘일네일링 벽체와 지하구조물 외벽을 합벽처리하는 사례가 많아지고 있으며, 이같은 지하외벽 일체식 쏘일네일링 공법은 기존의 지보공법과 비교해 볼 때 굴착면적을 최소화하고 시공성을 개선할 수 있는 특징이 있다. 또한 지하외벽 일체식 쏘일네일링 공법은 지하외벽의 단면 축소와 지하수에 의한 양압력의 영향에도 대처할 수 있는 장점이 있으나 아직까지는 이에 대한 연구가 미흡하여 보수적으로 설계되고 있는 실정이다. 이를 위해 본 연구에서는 실내모형실험을 통해 전면벽체의 강성에 따른 쏘일네일링 보강토체의 거동 및 네일의 두부에 작용하는 인발력을 분석하여 전면벽체의 강성에 따른 쏘일네일링 벽체의 파괴유형을 규명하고 사용상태 및 한계상태에서의 변위양상 및 네일 두부에서의 인장력 분포를 분석하였다. 또한 전면판의 강성이 쏘일네일링 벽체의 전체 안정성에 미치는 영향을 분석하였으며, 향후 전면벽체의 강성에 따른 지반-네일의 상호작용에 대한 모델개발에 필요한 기초적인 자료를 제공하고자 한다.

Abstract

Recently, there have been numerous attempts to expand the traditional temporary soil nailing system into a permanent wall. Two reasons for this include the soil nailed system's advantage of efficient and economic use of subgrade space and its ability to decrease the total construction cost. However, the systematic and logical design approach has not been proposed yet. The permanent soil nailing wall system, which utilizes precast concrete from soil nailing system, is already used in many countries, but the study of cast-in-place concrete facing or rigid walls in bottom-up construction of traditional soil nailing walls is imperfect and insufficient. In this paper, various laboratory model tests have been carried out to investigate the influence of parameters, including stiffness of the rigid wall to the soil nailing structure with respect to failure mode, displacement patterns and tensile forces at the nail head in several levels of load. Then, the variation of earth pressure distribution on the soil nailing wall, built with a rigid front plate, is sought through different levels of surcharge load and tensile forces at the nail head.

Keywords : Laboratory model tests, Permanent soil nailing wall system, Rigid wall

*1 Member, Professor, Dept. of Civil Engrg., Hong-Ik Univ. (htaek@wow.hongik.ac.kr)
*2 Member, Chief Engineer, Vniel Consultant Co., Ltd.
*3 Member, Manager, R&D Center, Halla Engrg. & Construction Corp.
*4 Member, Graduate Student, Dept. of Civil Engrg., Hong-Ik Univ.
*5 Engineer, Dohwa Consulting Engineers Co., Ltd.

1. Introduction

The soil nailed wall system has usually been applied for temporary pit excavation, the support of the cut slopes for road construction and the support of natural slopes next to houses since its first use in 1993 for temporary retaining walls in Korea. Also, this system can be utilized diversely in the underpinning of an existing building, the support of an existing retaining wall and the support of tunnel openings and fractured zones in shallow tunnels. Though the developments of the analysis theory and field and laboratory test have actively been progressed, the main stream of the study in Korea has been limited to the use of the soil nailed wall as a temporary retaining wall. Recently, unified soil nailed wall systems, which combine the soil nailed wall and the outside subgrade wall, are widely used as an economic and efficient means of subgrade excavation. This technology has the advantage of decreasing excavation area, minimizing the cross section of the outside subgrade wall, easing constructibility and sustaining positive ground water pressure. But the lack of study that has been performed for this particular technology makes unified soil nailed wall design a risky venture that requires the use of conservative assumptions. In this study with a laboratory model test, the following factors will be analyzed by the different front plate rigidity: 1) The behavior of the soil nailed reinforced body: 2) The pull-out force acting on the head of the nail; 3) The failure mode of the soil nailed wall; 4) The displacement of the wall at the allowable state and the limit state; and 5) The tensile force distribution at the nail head. Finally, basic data to develop a soil nailed interaction model will be suggested.

2. Laboratory Model Test

2.1 Introduction

The laboratory model test is conducted to examine the effect of the front plate rigidity on the soil nailed body by the length of the nail, the inserting angle of the nail and the surcharge load location. The apparatus includes a 1300mm long × 600mm wide × 600mm deep soil tube as shown in Fig. 1 (Kim et al., 2001; Yoo et al., 2001; Kim et al., 2002).

The soil used in this model is composed of Jumunjin standard sand and weathered granitic soil (with a ratio of 1:1.5) and the soil body is self-supported after excavation. Excavation will be performed in steps in consideration of the construction process of a soil nailed wall system in the field.

The size distribution curve of the soil is shown in Fig. 2 and its properties are shown in Table 1.

Two types of stainless bars will be used for the nails,

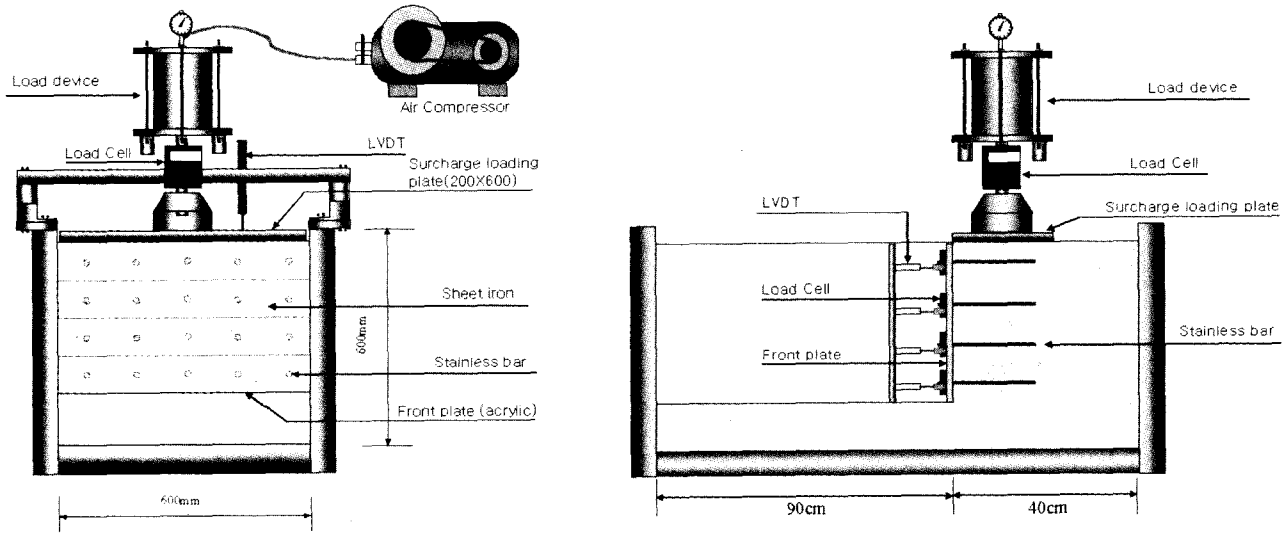

(a) A front of view

(b) A side of view

Fig. 1. The apparatus of laboratory model test

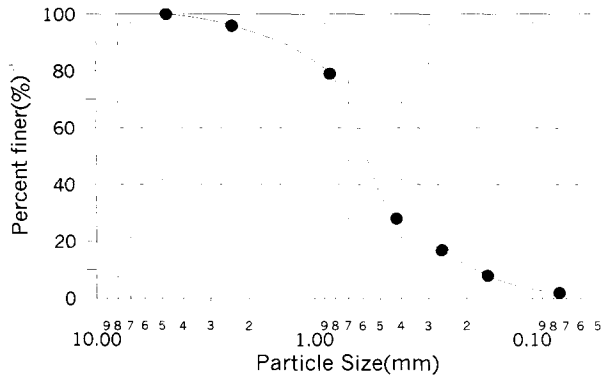

Fig. 2. The size distribution curve

the first type will be 200mm long and 3mm in diameter, and the second type will be 300mm long and 3mm in diameter. The 10mm long protrusion spiral line is used at the nail head to tie the front plate and the sheet iron together. The sheet iron, acting as a shotcrete in the field construction, has a dimension of 600mm long × 100mm wide with 0.2mm thickness. The acrylic plates (600mm long × 400mm wide with 2mm, 4mm and 6mm thickness) are used for the front plate and act as a rigid wall in the field construction. The surcharge loading plate is 600mm long × 200mm wide. Five LVDTs, one 5-ton capacity load cell (to measure load), four 3kg capacity load cells (to measure nail tension) are installed at the surcharge loading plate and the front plate. The vertical and horizontal displacement of the wall and tensile force on the nails, varying with excavation step and surcharge loading, are calculated through the data logger.

2.2 Test Procedure

The laboratory model tests are conducted based on static loading. Loading is applied at each excavation interval by an air compressor until failure of the wall occurs. To distribute the load on soil nailed body equally, the point load produced by the loading device is converted to a uniformly distributed load by a 600mm long × 200mm wide by 12mm thick plate. Also, the nail protruding through the front plate is connected to the front plate by fixed rings to measure the load acting on the nail and the front plate separately. The pull-out force acting on the nail head (located in the center of each stage), is measured by placing a load cell between the fixed ring. The load acting on the soil nailed body is measured by placing the load cell between the loading device and the loading plate. LVDTs located at the top of the stiffened loading plate and the center of each stage are used to measure vertical and horizontal displacement and settlement. Also, four different pull-out tests (pull-out speed of 1mm/min) with the strain control method are conducted for different nail diameters and nail installation depths. The eleven laboratory model tests (Table 2) and four pull-out tests (Table 3) were conducted to verify the effects of the front plate rigidity.

Fig. 3 shows the front plate and the soil body model

Table 1. The properties of the soil

Items	Values
Unit weight	1.49tf/m^3
Friction angle	34°
Cohesion	0.8tf/m^2
Limit of liquidity	28.8%
Limit of plasticity	17.6%

Table 2. Case of laboratory model tests

Case	Slope	Thickness of the front plate	Nail length	Nail diameter	Inserting angle of nail(°)	The front plate	The loading device
1	vertica	Unreinforcement					20cm × 60cm (b = 0cm)
2		–	20cm	3mm	0	–	
3		2mm	20cm	3mm	0	sheet iron+acrylic	
4		4mm	20cm	3mm	0	sheet iron+acrylic	
5		6mm	20cm	3mm	0	sheet iron+acrylic	
6	vertical	Unreinforcement					20cm × 60cm (b = 10cm)
7		sheet iron	30cm	3mm	0	sheet iron	
8		2mm	30cm	3mm	0	sheet iron+acrylic	
9		4mm	30cm	3mm	0	sheet iron+acrylic	
10		6mm	30cm	3mm	0	sheet iron+acrylic	
11	vertical	6mm	30cm	3mm	10	sheet iron+acrylic	20cm × 60cm (b = 10cm)

that was chosen for the laboratory model test. The nails were installed horizontally for Case 1 through Case 10 and at an angle (θ) of 10° for Case 11 as shown in Fig. 3 (b). The uniformly distributed loads were placed 10cm away (b=10cm) from the front plate with a nail length of 20cm for Case 1 through Case 5 and placed 10cm away (b=10cm) from the front plate with a nail length of 30cm for Case 6 through Case 11.

3. Test Results & Analysis

3.1 The Pressure at Failure with Increasing Front Plate Rigidity

Pressure versus vertical displacement of the wall

Table 3. Specifications and result of pull-out tests

No.	Insertion depth (cm)	Nail diameter (mm)	Nail length (cm)	Pull-out force (kgf)	Unit skin friction, q_s (t/m²)
1	15	3	30	0.53	0.18
2	25	3	30	0.87	0.31
3	15	5	30	1.22	0.26
4	25	5	30	2.04	0.43

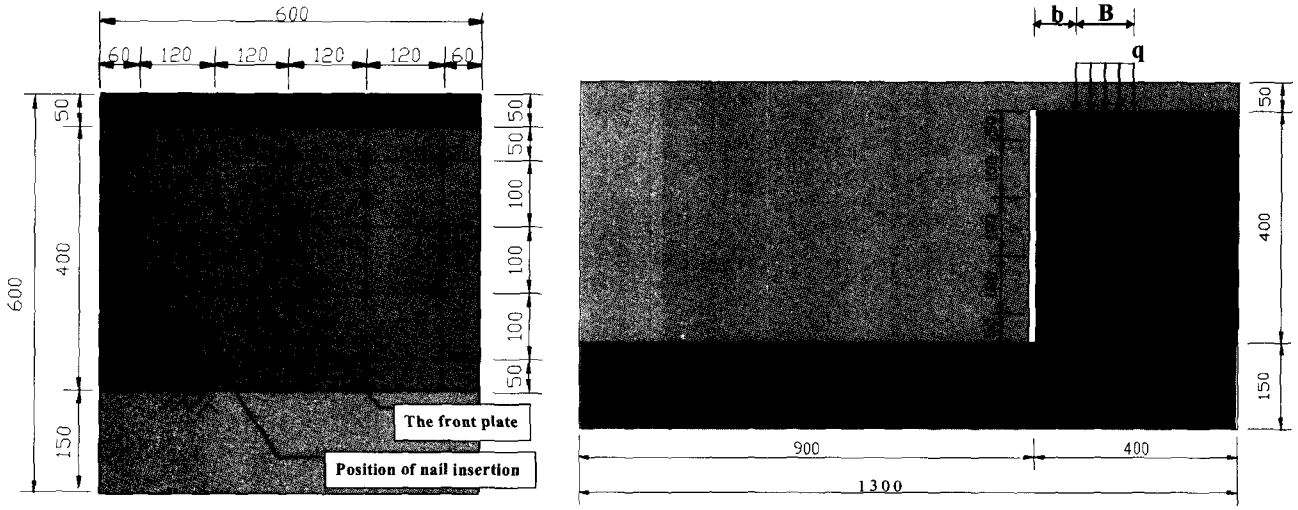

(a) A front of view (b) A side of view

Fig. 3. The front plate & the soil body model

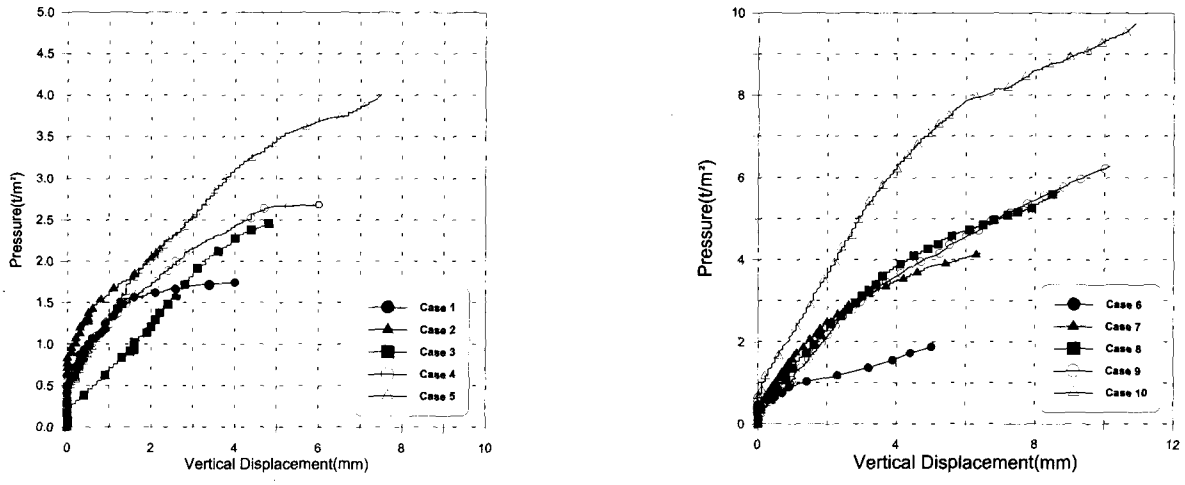

(a) Case 1 ~ Case 5 (b) Case 6 ~ Case 10

Fig. 4. Pressure versus vertical displacement of the wall relationships

Table 4. Failure pressure (q_f) with increasing front plate rigidity

Case	1	2	3	4	5	6	7	8	9	10
q_s (t/m²)	1.13	2.05	2.48	2.70	4.00	1.93	4.17	5.68	6.36	9.75

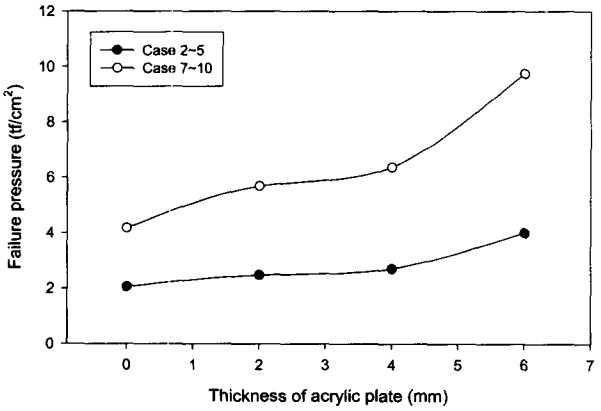

Fig. 5. The relationship of the failure pressure & the thickness of the front plate

relationships, which can examine failure pressure and displacement patterns until failure, are shown in Fig. 4. Also, the pressures at failure with increasing rigidity of the front plate are shown in Table 4.

In spite of the different load conditions and nail lengths in Cases 3, 4 and 5 and Cases 7, 8 and 9, the loads at failure are increased 1.09, 1.12, 1.16, and 1.72 times with increasing the thickness of the front facing plate from 2mm to 4mm, 2mm, and 6mm. These results are shown in Fig. 5.

3.2 Horizontal Displacement with Increasing Front Plate Rigidity

Fig. 6 shows the horizontal displacement at different depths along the front plate with 4 load stages from initial to the failure pressures (q_f), which are examined in Fig. 4.

The results from the tests shown in Fig. 6, Case 1 and Case 6, that are unreinforced show almost equal horizontal displacement increments at each depth from the top to the bottom of the plate at failure. Case 3 through Case 5 and Case 8 through Case 10, which have a front plate support, show larger horizontal displacement at the middle of the plate. Case 7 with a sheet iron (ductile plate) yields failure at relatively small displacements compared to the cases with the acrylic plate (rigid plate).

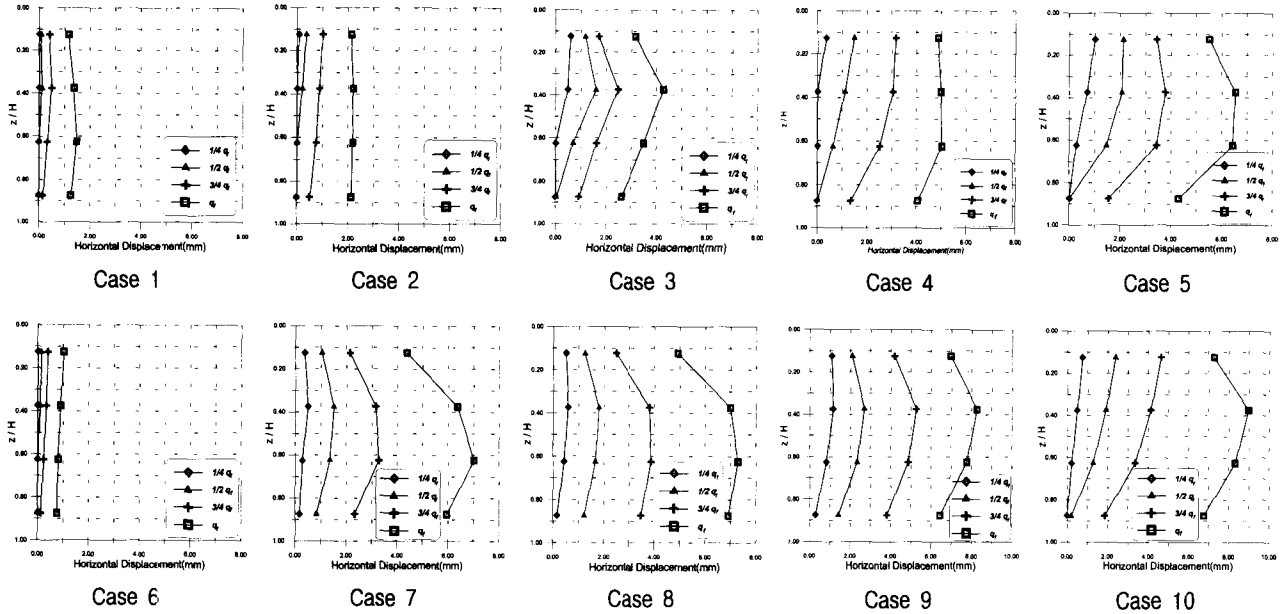

Fig. 6. The horizontal displacement with load stages

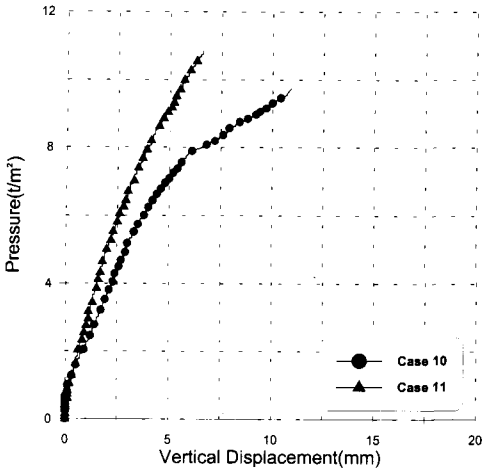

Fig. 7. The relationship of load versus vertical displacement (Case 10 & 11)

3.3 The Effect of the Nail Insertion Angle

Load versus vertical displacement relationships between Case 10 and Case 11 are shown in Fig. 7. All conditions are the same for Case 10 and Case 11 except the nail is inserted horizontally for Case 10 and inserted at an angle of 10° to the horizontal for Case 11.

The load at failure of Case 11 (10° nail insertion angle) is 11.18% larger than the load at failure of Case 10 (0° nail insertion angle) as shown in Fig. 7. Generally, with the same nail length, a nail insertion angle of 15° results in a more stable soil nailed wall than a soil nailed wall with a nail insertion angle of 0° by increasing failure load(Schlosser, 1991). This was proved by the comparison of case studies 10 and 11 in Fig. 7 above.

3.4 Earth Pressure Acting on the Soil Nailed Wall with Stiffened Front Facing Plate

3.4.1 Nondimensional Constant TN

Modified equation (1) is proposed to verify the earth pressure acting on the soil nailed wall with a rigid front plate. In this equation, $\cos\theta$ is eliminated because the nail is inserted horizontally, the overburden pressure term ($\gamma \cdot z$) is modified to include a surcharge load ($\gamma \cdot z + q$) and T_{max} is changed to T_i, which is the tension at the nail head (T_o) in each depth by assuming the maximum nail tension forces (T_{max}) is equal to the tension forces at the nail head.

$$TN = \frac{T_i}{\sigma_v \cdot S_H \cdot S_V} = \frac{T_i}{(\gamma \cdot z + q) \cdot S_H \cdot S_V} \quad (1)$$

Where, T_i = the nail tensile force at each depth (T_o),
γ = the total unit weight of the soil,
z = the nail depth,
q = the surcharge load,
S_H = the horizontal nail distance
S_V = the vertical nail distances.

Several reports on soil nailed wall technology including the Clouterre project in France have indicated that the ratio T_o/T_{max} is always less than 1 and the ratio is amplified by increasing the front plate rigidity. In this test, the maximum nail tensile force (T_{max}) is assumed equal to the tensile force at the nail head (T_o), because a highly rigid wall is used instead of a ductile wall (usually the case for soil nailed walls) and because the nail length is relatively short.

3.4.2 Earth Pressure Acting on the Soil Nailed Wall with Rigid Front Plate

Based on the assumptions in section 3.4.1, the tensile force at the nail head (T_o) as a function of depth in Cases 3, 4, 5, 8 and 10 is displayed in Fig. 8 to analyze earth pressure distributions acting on the rigid front plate along the soil nailed wall.

The *TN* distributions at the initial load state (q=1/2 q_f) in Fig. 8(a) show a similar trend with trapezoidal shaped earth pressure profiles. But, by increasing the load stages, all cases except Case 3 show an increasing *TN* at the bottom and yield a similar trend with triangular shaped earth pressure profiles at failure. This indicates that the trapezoidal shaped earth pressure profiles acting on the ductile wall are observed at initial load state, as proposed by Terzaghi & Peck and analyzed by several researchers, and that triangular shaped earth pressure profiles acting on the rigid wall are observed at failure(Juran, 1990).

Also, the load at the allowable limit ($\delta_{h(\max)}/H$ = 0.4%) in all cases is 51.4% of the maximum failure load (q_s), which is 25% ~ 50% of the failure load (q_f). This predicts that the *TN* versus *z/H* profile in this section is

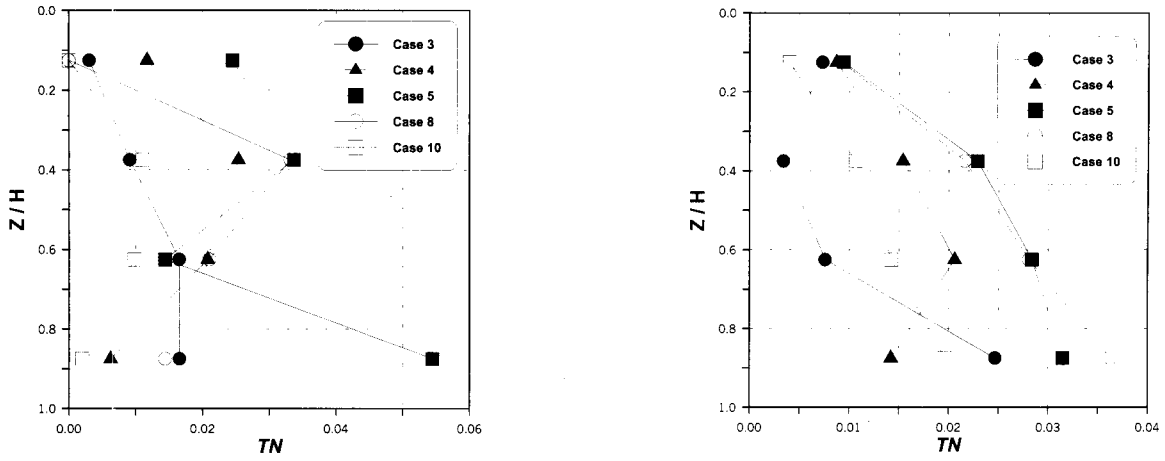

(a) Initial pressure stage (q=1/2q_f)

(b) Failure pressure stage (q=q_f)

Fig. 8. The tensile force at the nail head with the rigid front plate increasing

trapezoid in shape. These results conclude that if the allowable limit is ignored, then a triangular shaped earth pressure profile is acting on the rigid wall, and if the allowable limit is considered, then a trapezoidal shaped earth pressure profile is acting on the rigid wall.

4. Conclusions

This study examined failure load by various front plate rigidities, displacement at the wall and tensile forces acting at the nail head. Also, the earth pressure distributions acting on the soil nailed body were observed by analyzing the effect of various front plate rigidities. The results are summarized as follows.

(1) Pressure versus vertical displacement relationships of the soil nailed body with different front plate rigidity show similar trends. In spite of the different load conditions and nail length in Cases 3, 4 and 5 and Cases 7, 8 and 9, the loads at failure are increased 1.09, 1.12, 1.16, and 1.72 times with increasing the thickness of the front facing plate from 2mm to 4mm, 2mm, and 6mm. The case with front plate with 6mm thickness, which is front plate with relatively high rigidity, shows rapid increase of the failure load.

(2) In the case of displacement of walls with different front plate rigidities, Case 1 and Case 6, that are unreinforced show almost equal horizontal displacement increments at each depth from the top to the bottom of the plate at failure. Case 3 through Case 5 and Case 8 through Case 10, which have a front plate support, show larger horizontal displacement at the middle of the plate. Case 7, which has a sheet iron (ductile plate), yields failure at relatively small displacements compared to the cases with the acrylic plate (rigid plate).

(3) The load at failure of Case 11 (10° nail insertion angle) is 11.18% larger than the load at failure of Case 10 (0° nail insertion angle).

(4) In the case of earth pressure acting on the soil nailed wall with a stiffened front plate, the *TN* distributions at the initial load state (q=1/2 q_f) in Fig. 8(a) show similar trend with trapezoidal shaped earth pressure profiles. But, by increasing the load stages, all cases except Case 3 show an increasing *TN* at the bottom and yield a similar trend with triangular shaped earth pressure profiles at failure.

(5) In order to properly analyze the behavior of the soil nailed body and nail front plate interactions for different front plate rigidities in the future, laboratory and field tests are desired with various loads and various nail conditions.

Acknowledgements

This study was supported by the 2001 Hong-Ik University Academic Research Fund, and the authors express sincere gratitude for this support.

References

1. FHWA, *Manual for Design and Construction Monitoring of Soil Nail Walls*, Publication No.FHWA-SA-96-069, pp.63-136.
2. Juran, I., Elias, V. (1990), *Behavior and Working Stress Design of Soil Nailed Retaining Structure*, Performance of Reinforced Soil Structures, British Geotechnical Society, Thomas Telford, pp.207-212.
3. Kim, Hong-Taek, Kang, In-Kyu, Kwon, Young-Ho, Park, Si-Sam and Cho, Yong-Hoon (2002), "An Experimental Study of the Soil Nailed Wall Behavior with Front Plate Rigidity", *Proc. of the KGS Spring '02 National Conference*, pp.279-286 (in Korean).
4. Kim, Joon-Seok, Lee, Sang-Duk and Lee, Seung-Rae (2001), "An Experimental Study on Reinforcing Effects for Soil Structures Reinforced by Nail with an Anchor Shape", *Jour. of the KGS.* April, Vol.17, No.2, pp.103-111.
5. Schlosser, F. (1991), *Recommendations Clouterre / Soil Nailing Recommendations*, French National Rearch Project Report, No. FHWA-SA-93-026.
6. Yoo, Nam-Jae, Kim, Young-Gil, Park, Byung-Soo, Hong, Young-Kil (2001), "Centrifuge Model Tests on the Behavior and Failure Mechanism of Soil Nailing Systems Under Surcharges", *Jour. of the KGS.* Oct, Vol.17, No.5, pp.5-16.

(received on Apr. 22, 2002, accepted on Jun. 5, 2002)